Tunable plasmonic-crystal superlens for subwavelength imaging

A. Battula and S. C. Chen*
Department of Mechanical Engineering and Center for Nano and Molecular Science Technology, The University of Texas at Austin, Austin, Texas 78712, USA

(Received 1 October 2007; published 21 November 2007)

Here, we report a tunable plasmonic crystal (tPLC), where the polaritonic mode of a metallic array can be combined with the photonic mode of a hole array in a dielectric slab for achieving negative refraction and still possess an extra degree of freedom for tuning the tPLC as a superlens to operate at different frequencies. We numerically demonstrate the tunability of a single planar tPLC slab for subwavelength imaging (full width at half maximum, $0.38\lambda \sim 0.42\lambda$) by just varying the fluid in the hole array, thereby enabling the realization of ultracompact tunable superlens and paving the way for a class of unique lens.

DOI: 10.1103/PhysRevB.76.193408 PACS number(s): 42.25.Bs, 78.67.−n, 41.20.−q

A few decades ago, it was predicted that an isotropic medium with simultaneous negative electrical permittivity (ε) and magnetic permeability (μ) could display unique electromagnetic properties with "negative" index of refraction, which can be utilized for producing an image smaller than the wavelength. However, naturally occurring materials are not negative index materials (NIMs) and so specially engineered NIM called metamaterials have been proposed.[1–4] Yet, these metamaterials have a high probability of an unwanted resonance that could hinder ε and μ to be simultaneously negative in a frequency range.[5] Also in metamaterials, the negative index of refraction is determined by using an effective medium theory which would require that the operating wavelength is much larger than the size of the unit cell, and therefore it would be difficult to build a metamaterial device that can operate at optical or infrared (IR) frequencies.

An interesting alternative to the metamaterials could be the photonic crystal (PhC), which under proper conditions can act as a homogeneous medium with a negative index. The dispersion in a PhC can be described by the equifreqeucny surface (EFS) of the band structures of the PhC.[6] All-angle negative refraction was achieved at the lowest band of two-dimensional (2D) PhC, consisting of a square lattice of air holes in Si and the subwavelength image formed is in the near field of PhC.[7] It was observed in Ref. 8 that the near-field subwavelength imaging is mainly due to the self-collimation effect and near-field scattering apart from the negative refraction effect that might also take place. Nevertheless, far-field imaging and focusing have been achieved in the lowest (or valence) band for a 2D square lattice of dielectric coated metallic core cylinders immersed in air background.[6] Also, surface termination within a specific cut of the triangular array of dielectric bars would excite surface waves at the interference between air and PhC dielectric bar, which would allow the reconstruction of evanescent waves for a better focus and transmission.[9] Similarly, a superlens made of planar metal film was demonstrated for subdiffraction limited optical imaging.[10]

Optical systems synthesized by using fluids are called optofluidics. A number of microfluidic devices based on PhC have been reported. One such PhC sensing device is based on a high-Q cavity resonance shift due to the various analytes in the cavity.[11] Recently, it was reported that by introducing coupled defects into the PhC waveguide, the sensing of biomaterials such as DNA, which fills the defects, was made possible by measuring the associated changes in the transmission of the PhC.[12,13]

In this Brief Report, we propose a 2D tunable plasmonic crystal (2D tPLC) that is considered to have a triangular array of metallic cylinders in a Si ($\varepsilon=12$) substrate which also has graphene array holes, as shown in the inset of Fig. 1(a). The lattice constant of the metallic cylinders is a, whereas the lattice constant of the holes is $a/\sqrt{3}$. The metallic cylinders have a radius (r_a) of $0.3a$ and the holes have a radius (r_b) of $0.2a$. The holes can be filled with different organic liquids to have various dielectric constants that would subsequently shift the frequency range for negative refraction. The present study has considered the holes to be filled with either air ($\varepsilon=1$), tetrachloromethane (CCl_4; $\varepsilon=2.23$), or dichloroethane ($C_2H_4Cl_2$; $\varepsilon=10.10$). Electromagnetic response (ε) of each metallic cylinder is assumed to be dispersive in IR and can be described by a free-electron model. The lattice constant a is taken to be 375 nm and the plasma frequency ω_p is 1.25×10^{16}, which is close to the ω_p of gold in the IR range of 1.4–1.65 μm. We report only the transverse electric (TE) mode (in-plane electric field, x-y) propagation bands inside the 2D tPLC since for the transverse magnetic mode, we found no superlensing effect. The TE mode photonic band structure (PBS) can be obtained by solving Maxwell's equations as an eigenvalue problem for H_z, which satisfies the phase-shifted periodic boundary condition as given by $H_z(\vec{r}+\vec{a})=H_z(\vec{r})e^{i\vec{k}\vec{r}}$, with $\vec{a}$ as a vector connecting the opposite edges of the unit cell and $\vec{k}$ as a Bloch wave number that belongs to the irreducible Brillouin zone.[14] Numerical calculations were carried out by using a commercially available finite element software COMSOL 3.2a.[15]

Figure 1(a) shows the TE mode PBS for the 2D tPLC with the holes filled with different fluids. When the holes are filled with air, there is a complete photonic band gap between the second and third bands, i.e., for $\Omega(=\omega a/2\pi c)$ in the range of 0.31–0.41. The second band has a convex shape around the Γ point, which would give a homogeneous negative refraction in the PhC[7,8] and will be shown later. When the holes are filled with CCl_4, then the resulting PBS would look similar to the previous one except for the complete band gap that would now occur for Ω in the range of 0.305–0.37. However,

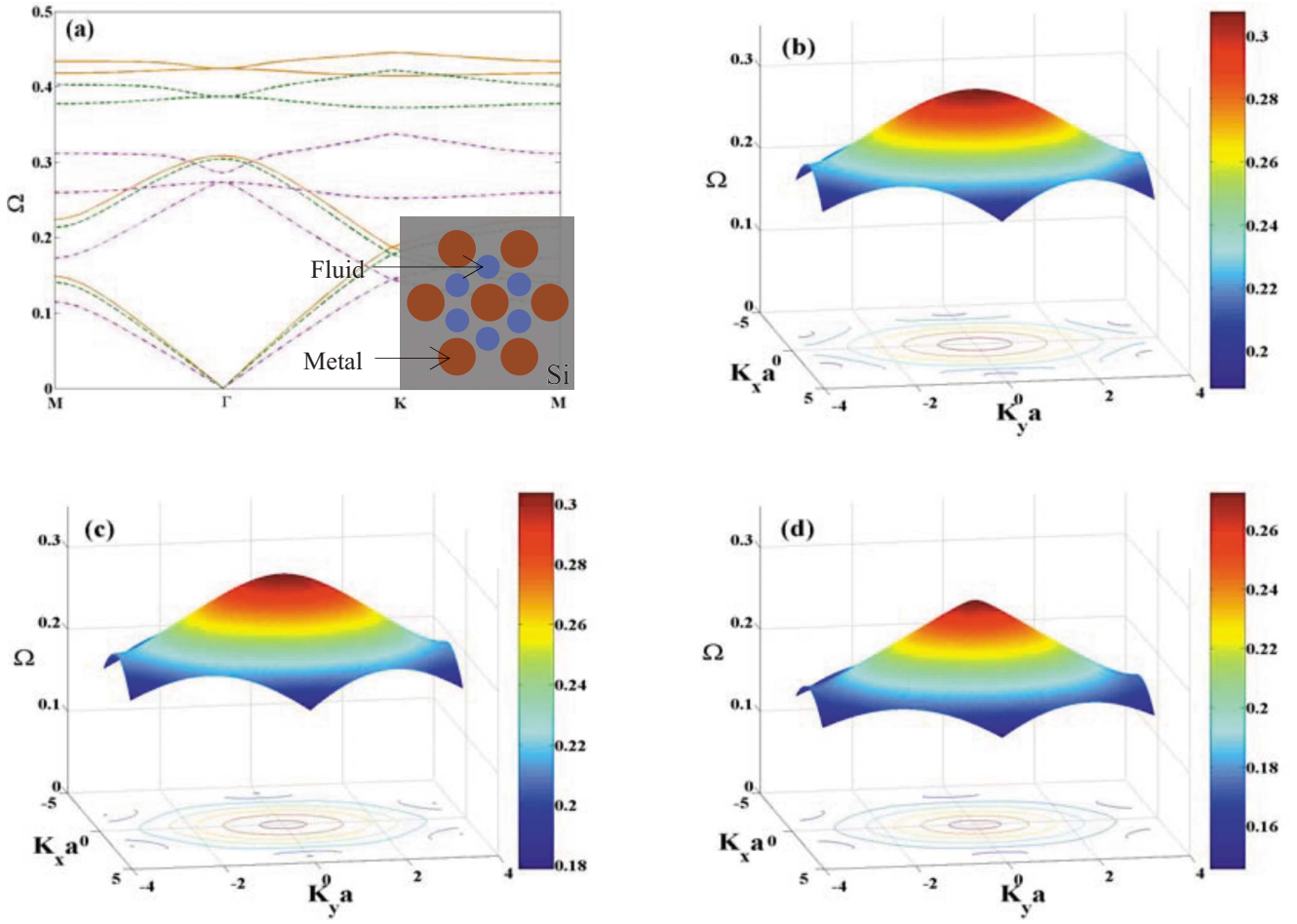

FIG. 1. (Color online) (a) TE mode PBS for a 2D tPLC (schematic figure in the inset) filled with air (solid lines), CCl_4 (dashed line), and $C_2H_4Cl_2$ (dashed dot line) and EFS for the second band of TE mode with the holes filled with (b) air, (c) CCl_4, and (d) $C_2H_4Cl_2$.

by changing the fluid in the hole with a higher dielectric constant, like with $C_2H_4Cl_2$, the resulting PBS would change with the complete band gap occurring now between the third and fourth bands for Ω in the range of 0.275–0.285. The second band would still be convex around the Γ point. Figure 1(b) shows the EFS for the second band of the 2D tPLC with the holes filled with air. EFS basically consists of allowed propagation modes within the Brillouin zone of the tPLC at a specific frequency. Most of the frequency contours in Fig. 1(b) are isotropic with circular shapes having a center around the Γ point. Thus, when a plane wave is incident from vacuum onto the present tPLC, the refracted angle would be linearly proportional to the incident angle. This would then help to have far-field images. For every chosen $\vec{k}$, the corresponding $\vec{v}_g$ will be normal to the EFS at that point and will point toward increasing frequency. Hence, $\vec{v}_g$ at any point on the circular EFS contour is collimated with $\vec{k}$, indicating that the PhC slab medium behaves like an effective homogeneous medium. Figure 1(b) also shows that for a Ω region of 0.225–0.305, the EFS contours are moving inward with increasing frequency. This would then result in $\vec{v}_g \cdot \vec{k} < 0$, which is equivalent to $\vec{S} \cdot \vec{k} < 0$ since it has been shown analytically that for an infinite PhC system $\vec{v}_g$ coincides with the energy velocity $(\vec{S})$.[16] $\vec{S} \cdot \vec{k} < 0$ is of particular necessity for a left-handed material (LHM).[17] In a LHM $\vec{k}$, $\vec{E}$, and $\vec{H}$ form a left-handed set of vectors, which could then give a negative refraction. Therefore, the 2D tPLC with the holes filled with air can be considered as a homogeneous medium with an effective negative index of refraction (n_{eff}) for Ω in the range from 0.225 to 0.305. Similarly, Fig. 1(c) shows that the EFS contours of the second band for 2D tPLC with the holes filled with CCl_4 which is the same as the previous case except for negative refraction is happening in a different Ω region (0.215–0.30). When the holes are filled with an even higher dielectric constant of $C_2H_4Cl_2$, the EFS contours of the second band would still have circular shapes [Fig. 1(d)] and the negative refraction happens at a lower Ω range of 0.175–0.27. Also, it can be noted from Figs. 1(b)–1(d) that the EFS contour shapes become more of a conical shape from hemispherical shape as the dielectric constant in the hole increases.

The main challenge for perfect superlensing is to find a lens structure with a matching n_{eff} that will then have no reflections during the imaging process.[9] Figure 2 shows the n_{eff} variation with respect to Ω along two different propagation directions of ΓM and ΓK in the Brillouin zone of the 2D tPLC for various fluids filling the holes. The n_{eff} for each fluid in the hole is the same in both ΓM and ΓK directions for most of their respective second band frequency range.

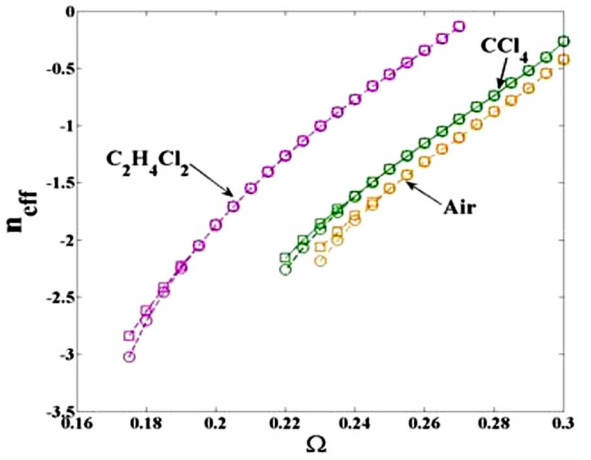

FIG. 2. (Color online) Effective refractive index (n_{eff}) of a 2D tPLC for the second band in ΓM (circles) and ΓK (square) directions of propagation with the holes filled with air (dashed dot line), CCl_4 (solid line), and $C_2H_4Cl_2$ (dashed line).

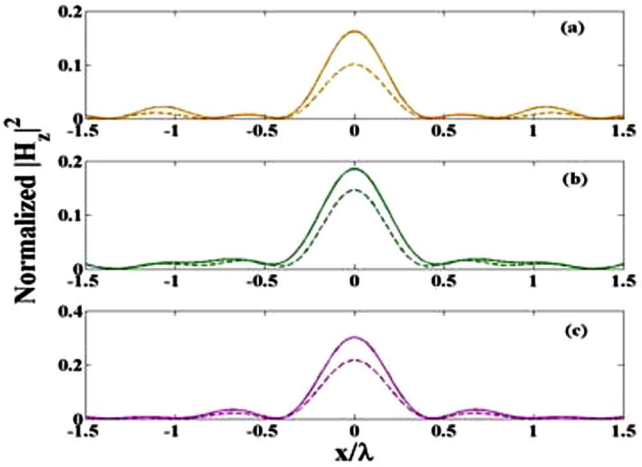

FIG. 4. (Color online) The holes of 2D tPLC are filled with (a) air ($\Omega=0.27$), (b) CCl_4 ($\Omega=0.26$), and (c) $C_2H_4Cl_2$ ($\Omega=0.23$). Solid line is for the free-electron model metal cylinder and the dashed line is for the gold cylinder.

Also, Fig. 2 suggests that at a particular Ω, the n_{eff} can be tuned to different negative values and to different Ω at a particular n_{eff} by just varying the dielectric constant of the fluid in the holes.

A typical H_z field distribution across the planar 2D tPLC with different fluids in the holes is plotted in Figs. 3(a)–3(d) for a source having diameter a and placed at different distances d. Figure 3(a) shows the H_z pattern with holes filled with air for a source at $\Omega=0.27$ (tPLC has $n_{\text{eff}}\approx -1$, Fig. 2) and is placed on top of the slab at $d=2a$. A high quality

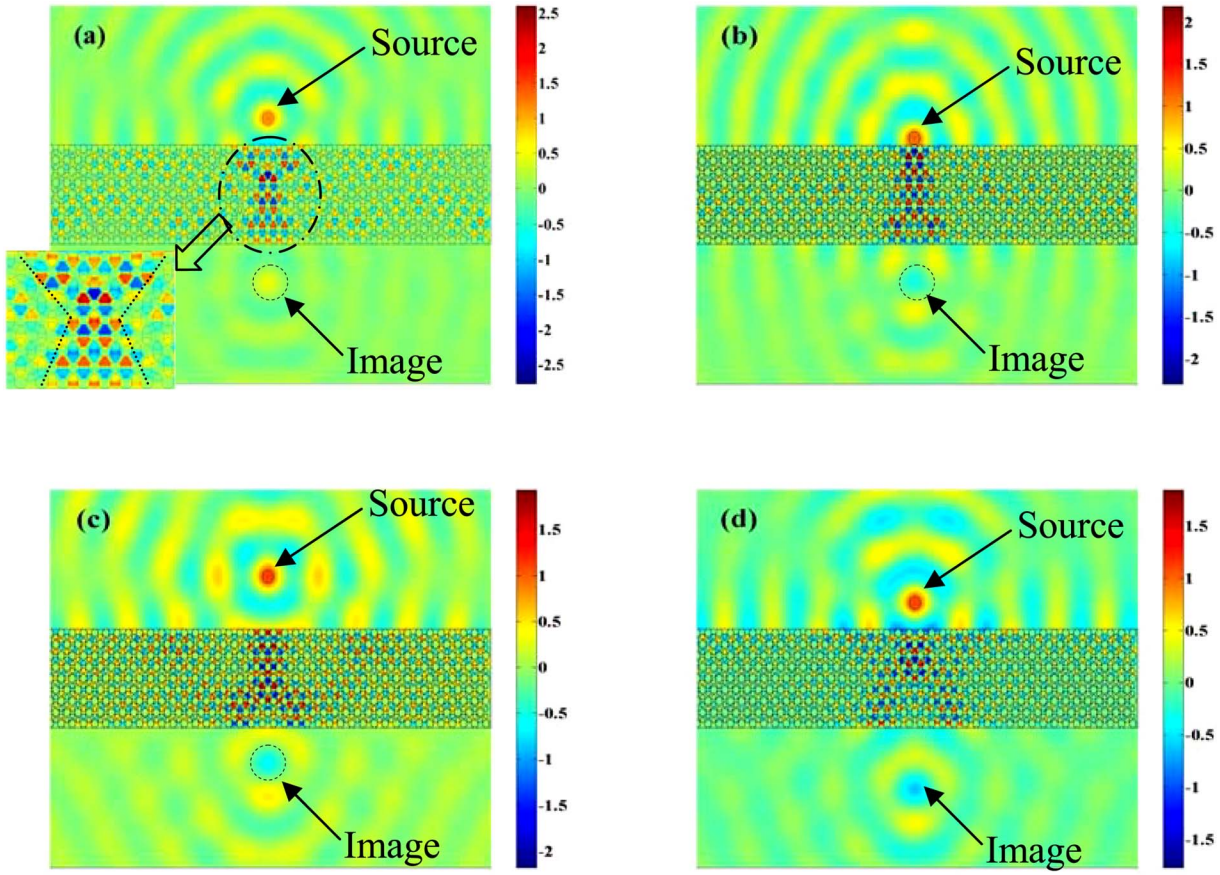

FIG. 3. (Color online) Snapshot of the H_z field produced by a point source placed on the top of the 2D tPLC slab at a distance (a) $d=2a$ ($\Omega=0.27$) with the holes filled with air, (b) $d=0.55a$ ($\Omega=0.26$)) with the holes filled with CCl_4, (c) $d=4a$, and (d) $d=2a$ ($\Omega=0.23$) with the holes filled with $C_2H_4Cl_2$.

image on the opposite side of the PhC slab is observed along with a focusing region in the middle of the slab [inset of Fig. 3(a)], which is in accordance with the wave-beam geometric optics. The rays diverging from the source would negatively refract at the top surface of the slab and converge at a point within the slab. The rays would then diverge from the focus region in the slab and then negatively refract again at the bottom surface of the slab to converge and form a final image outside the slab. Figure 3(b) shows the superlensing effect at a different frequency when the 2D tPLC is filled with CCl_4. The source is at $\Omega=0.26$ (tPLC has $n_{\text{eff}}\approx-1$, Fig. 2) and placed at $d=0.55a$ with the image formed having a full width at half maximum (FWHM) of 0.41λ. In order to further clarify whether the superlensing effect of the present 2D tPLC slab is in complete accordance with the geometric optics, the dependence of image distance on the source distance is explored. Figures 3(c) and 3(d) show the H_z field pattern across a planar 2D tPLC slab with the holes filled with $C_2H_4Cl_2$ along with a source having $\Omega=0.23$ (tPLC has $n_{\text{eff}}\approx-1$, Fig. 2) at distances $4a$ and $2a$ from the top of the slab, respectively. It is seen that with a change in the source distance from the slab, the image distance changes too. The FWHM of the images are 0.41λ in Fig. 3(c) and 0.40λ in Fig. 3(d). In addition, Fig. 3(d) shows the existence of surface waves (alternate blue and yellow spikes) or surface plasmons on the top surface of the tPLC slab.

Figures 4(a)–4(c) show the normalized intensity versus the lateral direction (given in terms of wavelength) at the image plane with the holes filled with (a) air, (b) CCl_4, and (c) $C_2H_4Cl_2$. The object diameter is a, which in terms of the source wavelength is $\Omega\lambda$ and is placed at $d=2a$ from the top surface of the planar tPLC slab. Figure 4(a) shows the image intensity plots for a source at $\Omega=0.27$ (or $\lambda=a/\Omega\approx1.4$ μm) and for when the cylinder in the tPLC is either a free-electron model metal or gold with a dielectric constant[18] having absorption. FWHM for both cylinder cases is 0.38λ. For a tPLC with holes filled with CCl_4, Fig. 4(b) shows that a source at $\Omega=0.26$ (or $\lambda\approx1.44$ μm) will have a FWHM of 0.42λ when the cylinders in tPLC are free electron-model metal and a FWHM of 0.38λ when the cylinders are gold. For a tPLC with holes filled with $C_2H_4Cl_2$, Fig. 4(c) shows that an object source at $\Omega=0.23$ (or $\lambda\approx1.63$ μm) will have an image intensity with FWHM of 0.4λ for both types of cylinders. The dielectric response of gold in the IR range has an imaginary part that is 2 orders of magnitude lower than the real part. Hence, the imaging characteristics would not change with very low absorption but the FWHM of the image intensity might change by a small extent.[6,19]

In conclusion, it is shown that the present 2D tPLC has an extra degree of freedom that can be used for tuning the tPLC to different n_{eff} at a particular Ω and to a different Ω at a particular n_{eff}. In addition, the superlensing by the tPLC can be realized with $n_{\text{eff}}\sim-1$ at different frequencies, which could then be used for imaging objects of different sizes. Also, it is shown that an object with a smaller size in comparison with the wavelength and when placed far from the lens, a subwavelength image can still be achieved by using the present tPLC model but with the holes filled with a higher dielectric constant fluid. Furthermore, a higher resolution image of an object that is placed closer to the lens can be achieved by using the present tPLC model but with a lower dielectric constant fluid in the holes of tPLC. Also, there is an analogy between the plasmonic modes of the present PLC and the lattice vibration modes of a solid crystal. The lattice vibrations of a solid can be tuned by having distinctive atoms in the crystal and it proved instrumental in the field of solid state physics. In a similar way, the current work would make a significant contribution to the emerging field of "tunable plasmonic solids."

This work was supported by research grants from the U.S. National Science Foundation (CMMI0600104, CMMI0609345, and CBET0243160). The authors appreciate computer support from Intel's Higher Education Program.

*Corresponding author; scchen@mail.utexas.edu

[1] J. B. Pendry, A. J. Holden, D. J. Robbins, and W. J. Stewart, J. Phys.: Condens. Matter **10**, 4785 (1996).
[2] D. R. Smith, W. J. Padilla, D. C. Vier, S. C. Nemat-Nasser, and S. Schultz, Phys. Rev. Lett. **84**, 4184 (2000).
[3] R. A. Shelby, D. R. Smith, and S. Schultz, Science **292**, 77 (2001).
[4] A. A. Houck, J. B. Brock, and I. L. Chuang, Phys. Rev. Lett. **90**, 137401 (2003).
[5] C. M. Soukoulis, M. Kafesaki, and E. N. Economou, Adv. Mater. (Weinheim, Ger.) **18**, 1941 (2006).
[6] X. Zhang, Phys. Rev. E **71**, 037601 (2005).
[7] C. Luo, S. G. Johnson, and J. D. Joannopoulos, Phys. Rev. B **65**, 201104(R) (2002).
[8] Z-Y. Li and L-L. Lin, Phys. Rev. B **68**, 245110 (2003).
[9] R. Moussa, S. Foteinopoulou, L. Zhang, G. Tuttle, K. Guven, E. Ozbay, and C. M. Soukoulis, Phys. Rev. B **71**, 085106 (2005).
[10] N. Fang, H. Lee, C. Sun, and X. Zhang, Science **308**, 534 (2005).
[11] M. Loncar, A. Scherer, and Y. Qiu, Appl. Phys. Lett. **82**, 4648 (2003).
[12] H. Kurt and D. S. Citrin, Appl. Phys. Lett. **87**, 041108 (2005).
[13] T. Hasek, H. Kurt, D. S. Citrin, and M. Koch, Appl. Phys. Lett. **89**, 173508 (2006).
[14] J. D. Joannopoulos, R. D. Meade, and J. N. Winn, *Photonic Crystals: Modeling the Flow of Light* (Princeton University Press, Princeton, NJ, 1995).
[15] *COMSOL 3.2 Reference Manual* (Comsol AB, Stockholm, 2005).
[16] K. Sakoda, *Optical Properties of Photonic Crystals* (Springer, Berlin, 2001).
[17] S. Foteinopoulou and C. M. Soukoulis, Phys. Rev. B **67**, 235107 (2003).
[18] E. D. Palik, *Handbook of Optical Constants of Solid* (Academic, Orlando, 1985).
[19] X. Wang and K. Kempa, Phys. Rev. B **71**, 233101 (2005).